In the proceedings of the 1996 IEEE
Robotics and Automation Conference,
Minneapolis Minnesota, April 1996

# Tactile Sensing and Stiffness Control with Multifingered Hands

**Jae S. Son and Robert D. Howe**

Harvard University, Division of Applied Sciences
Pierce Hall, Cambridge, Massachusetts, 02138 USA
Email: jae@hrl.harvard.edu

## *Abstract*

*In this paper we analyze and experimentally measure the benefits of tactile sensing for stiffness control in the presence of uncertainty. There are two parts of the manipulation process where tactile information is helpful: determining the initial object pose as the fingers close to grasp, and tracking the object as it rolls and slides against the fingers during manipulation. The paper begins with an analysis of uncertainty associated with the initial orientation of a grasped object. We then review the object stiffness control algorithm [Salisbury 1985], and derive an expression for the errors in the commanded stiffness based on object orientation uncertainty. Experimental execution of a peg insertion task demonstrates that tactile sensing can effectively determine the initial orientation of the object. Tactile sensing can also be used to track object rolling, but update rates are slow, which can limit the maximum stiffness.*

## 1. Introduction

In order for robots to move out of the factory and into our daily lives, they must adapt to unstructured environments. Tactile sensing promises to increase the dexterity of robot hands by providing information about the mechanical state at the finger-object interface. One type of information that is particularly important is the contact location, and its motion as the grasped object rolls or slides against the finger tip during manipulation. Recent research on the use of tactile information in manipulation has demonstrated the capability of using this contact location in real-time control. Berger and Khosla [1991] and Chen et al. [1995] used tactile array sensors to track object edges in sliding. Maekawa et al. [1995] and Nicolson [1995] used tactile information to reorient objects by rolling them between the finger tips.

In this paper we examine methods of using contact information to improve the performance of object stiffness control with multifingered hands. Stiffness control provides a means to modulate the mechanical impedance of a grasped object. A number of studies have demonstrated that impedance control permits effective robotic execution of certain tasks, and several algorithms have been proposed for controlling a robot hand to achieve a desired impedance of a grasped object [e.g., Salisbury 1985; Cutkosky and Kao 1989].

The stiffness control algorithm attempts to make the grasped object act as if suspended by a set of springs and dampers. The controller senses displacement of the object from its desired location and orientation, and uses the fingers to generate proportional restoring forces and torques. Without tactile sensing, the stiffness controller can only sense object displacements through motions at the finger joints. Therefore, tactile sensing can enhance the performance of stiffness control by providing object-finger contact location information. There are two parts of the manipulation process where tactile information is helpful: determining the initial object pose as the fingers close to grasp, and tracking the object as it rolls and slides against the fingers during manipulation.

In this paper we analyze and experimentally measure the benefits of tactile sensing for stiffness control in the presence of uncertainty. To provide a focus, we consider peg-in-hole insertion as the prototype for a range of dexterous manipulation tasks involving contact between the environment and the grasped object. We begin with an analysis of the uncertainty in the initial orientation of a grasped object, based on friction and object-width to finger-tip-radius ratio. Then we review the stiffness control algorithm, and calculate the errors in the actual stiffness of the grasped object based on object orientation uncertainty. Finally, we look at rolling manipulation, and present the results of an experimental execution of the peg insertion task.

## 2. Orientation uncertainty from friction

Uncertainty in object orientation after grasping can arise from friction between the fingers and the object. To illustrate this uncertainty, consider an unconstrained object with parallel flat sides at a skewed orientation as two fingers come together to grasp it. If there is no friction, the object will slide against the fingers and reorient so that its surfaces are perpendicular to the line between the fingers. The object orientation may then be inferred from the positions of the finger tips, i.e. from joint angle measurements. If friction is present, however, sliding will stop before this condition is reached. This static equilibrium occurs when the grasp force, which is directed between the finger-object contact points, falls within the friction cones centered about the object's surface normals. For "point contact" finger tips whose radius is small compared with the size of the object, the range of stable object orientations is determined by the friction cone angle $\psi = \tan^{-1}\mu$, where $\mu$ is the coefficient of friction. For fingers with finite radius, the limiting equilibrium angle of the object also depends on the ratio of object-width to the finger-tip-radius along with the friction coefficient.

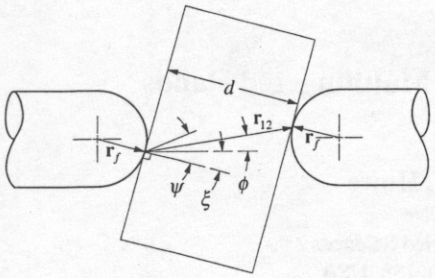


Figure 1. Variables used in calculating the object rotational uncertainty for cylinderical finger tips and a parallel-sided object.

For cylinderical finger tips grasping a parallel, flat sided object, Figure 1 shows the situation in the plane containing the finger tip centers and the finger-object contact points. For grasp stability

$$\psi \geq \phi + \xi \qquad (1)$$

where $\xi$ is the object orientation angle and $\phi$ is the grasp force angle, both defined with respect to the horizontal. The relationship between object orientation and grasp force orientation is

$$\phi = \sin^{-1}\left(\frac{2r_f \sin\xi}{r_{12}}\right) \qquad (2)$$

where the distance between the contact points is in the plane of the grasp vector, $r_f$ is the finger tip radius, and $d$ is the object width. This expression is immediately applicable to the peg insertion experiments described below; extension to objects with non-parallel sides is accomplished by considering when the grasp force vectors at each contact point pass into the friction cones.

Figure 2 shows the limiting object orientation angle calculated from these relationships as a function of the coefficient of friction, for various values of the object-width to finger-tip-radius ratio. For pointed finger tips ($\mathbf{r}_f << d$) the orientation uncertainty is simply the friction cone angle, and for parallel-jaw grippers with flat fingers ($\mathbf{r}_f >> d$), the uncertainty is zero. In a typical dexterous manipulation task, a robot hand might manipulate objects about as wide as the finger tips ($\mathbf{r}_f \approx d$) with a coefficient of friction of about 1, resulting in maximum object orientation uncertainty of ±15–20 degrees. Next, we consider the effects of such large uncertainties on object stiffness control.

## 3. Stiffness controller

### 3.1 Control law

From the many proposed schemes for coordinating the control of multifingered hands, we have selected Salisbury's Cartesian object stiffness control [Salisbury 1985] for its simplicity and immediate applicability to the peg insertion task. Further analysis of this controller and its limits can be found in [Son and Howe 1995]. Cartesian object stiffness control permits the specification of a center of compliance (CC) and the magnitudes of the object stiffness in each direction about that CC in Cartesian coordinates. By measuring the difference

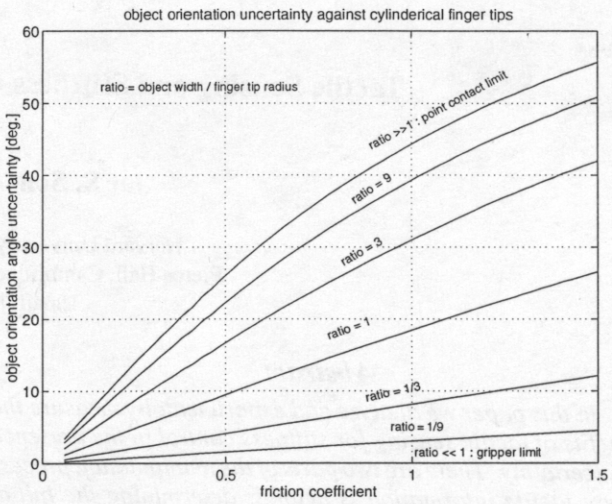


Figure 2. Object orientation uncertainty as a function of the friction coefficient for a variety of object-width to the finger-tip-radius ratios.

between the desired and actual CC locations, a restoring force on the object is calculated through the stiffness matrix,

$$\mathbf{f}_{obj} = \mathbf{K}_{obj}\delta\mathbf{x}_{obj}, \qquad (3)$$

where $\mathbf{f}_{obj}$ is the net force on the object, $\mathbf{K}_{obj}$ is the desired stiffness matrix at the CC, and $\delta\mathbf{x}_{obj}$ is the object location error or the difference between the desired and actual CC locations. In practice, the object force is augmented to include grasp force and gravity compensation terms. The object force is mapped to the finger tips, $\mathbf{f}_{tip}$, with the transpose of the grasp matrix $\mathbf{G}^T$

$$\mathbf{f}_{tip} = \mathbf{G}^T\mathbf{f}_{obj}. \qquad (4)$$

The finger tip forces are then mapped to the required joint torques, $\tau$, with the transpose of the Jacobian matrix, $\mathbf{J}^T$, and combining (3) and (4) yields

$$\tau = \mathbf{J}^T\mathbf{f}_{tip} = \mathbf{J}^T\mathbf{G}^T\mathbf{K}_{obj}\delta\mathbf{x}_{obj}. \qquad (5)$$

To determine the object position error, we start with measured joint angles, $\mathbf{q}$, then calculate the location of the contact between the finger-tip and object from the manipulator forward kinematics, $f$, which includes the contact kinematics. Next, the object location is computed from the grasp kinematics, $g$, which relate the contact location to the CC location

$$\mathbf{x}_{obj} = g(f(\mathbf{q})). \qquad (6)$$

Both the manipulator kinematics and the grasp kinematics must account for changes in the contact location due to rolling or sliding of the object against the finger tips. This is where models of rolling and sliding behavior or tactile sensing of contact location, play a vital role. Combining the above relations, the explicit control law is

$$\tau = \mathbf{J}^T\mathbf{G}^T\mathbf{K}_{obj}(\mathbf{x}_{obj,des} - g(f(\mathbf{q}))). \qquad (7)$$

### 3.2 Stiffness error

We wish to derive a relation that describes the stiffness errors caused by inaccurate determination of contact locations

and initial object position and orientation. First, we consider the force that is actually generated in response to object displacements. This may contain several sources of error. We can explicitly enumerate these errors by combining (4) and (5) to find

$$\mathbf{f}_{obj} = \mathbf{G}^{-T}\mathbf{f}_{tip} = \mathbf{G}_{act}^{-T}\mathbf{J}_{act}^{-T}\tau_{act}, \qquad (8)$$

where the subscript "act" refers to the actual physical situation, as opposed to the calculated quantities based on joint angle measurements and kinematic relations. We can describe the actual torque, $\tau_{act}$, as composed of the desired component, $\tau_{des}$, calculated from (7) above, plus a disturbance term, $\tau_{disturbance}$, due to joint-level friction, motor torque ripple, D/A quantization, amplifier noise, and other actuation defects. Combining (5) with (8) yields

$$\begin{aligned}\mathbf{f}_{obj} &= \mathbf{G}_{act}^{-T}\mathbf{J}_{act}^{-T}(\tau_{disturbance} + \tau_{des}) \\ &= \mathbf{G}_{act}^{-T}\mathbf{J}_{act}^{-T}\tau_{disturbance} + \mathbf{G}_{act}^{-T}\mathbf{J}_{act}^{-T}\mathbf{J}_{calc}^{T}\mathbf{G}_{calc}^{T}\mathbf{K}_{obj}\delta\mathbf{x}_{obj}.\end{aligned} \qquad (9)$$

If there are no kinematic errors, then $\mathbf{J}_{act} = \mathbf{J}_{calc}$ and $\mathbf{G}_{act} = \mathbf{G}_{calc}$, and the joint torques will be accurately mapped to the object force. Errors, particularly in contact location, will degrade the mapping, and incorrect object forces will result. The magnitudes of these errors will vary greatly with the details of the grasp and joint configuration; explicit values for specific situations may be calculated with this relation.

Disturbance torques such as friction, motor torque ripple, and amplifier gain variation may sometimes be modeled or directly sensed and corrected, and improved manipulator designs can help limit these disturbances. However, incorrect determination of contact and object locations cannot be corrected in this manner. If we neglect the disturbance torques, the force on the object reduces to

$$\mathbf{f}_{obj} = \mathbf{G}_{act}^{-T}\mathbf{J}_{act}^{-T}\mathbf{J}_{calc}^{T}\mathbf{G}_{calc}^{T}\mathbf{K}_{obj}\delta\mathbf{x}_{obj}. \qquad (10)$$

This equation shows that the actual stiffness matrix $\mathbf{K}_{act}$ is the product of the desired stiffness matrix $\mathbf{K}_{obj}$ and a stiffness error matrix, $\mathbf{E}$, or

$$\mathbf{K}_{act} = \mathbf{E}\mathbf{K}_{obj} = \mathbf{G}_{act}^{-T}\mathbf{J}_{act}^{-T}\mathbf{J}_{calc}^{T}\mathbf{G}_{calc}^{T}\mathbf{K}_{obj}. \qquad (11)$$

The $\mathbf{E}$ matrix provides a measure of object stiffness deviations generated by improper mapping of contact and object locations. If the kinematics are correctly described by the $\mathbf{G}_{calc}^{T}$ and $\mathbf{J}_{calc}^{T}$ matrices, then $\mathbf{E}$ will be an identity matrix and the actual stiffness matrix will agree with the desired one. The divergence from an identity matrix describes the effects of the kinematic errors, independent of the particular $\mathbf{K}_{obj}$ values. The actual stiffness matrix can then be found by pre-multiplying any specified desired stiffness matrix $\mathbf{K}_{obj}$ by $\mathbf{E}$.

The calculation of $\mathbf{E}$ for a particular example will demonstrate the nature of the resulting stiffness errors. Since our manipulator works in a plane, the object forces and displacements are $\mathbf{f}_{obj} = [f_x, f_y, \tau, f_g]^T$ and $\delta\mathbf{x}_{obj} = [x, y, \theta, 1]^T$ respectively, and $\mathbf{K}_{obj}, \mathbf{E} \in \Re^{4\times4}$. Two planar fingers, with radius of 1.5 cm, are grasping a parallel flat sided object of width 2 cm, as shown in Figure 1. The object stiffness controller is commanded to place the CC symmetrically between the finger tips. In the absence of tactile information about the actual orientation of the object, the controller must assume $\xi = \phi = 0$. If the actual object orientation is 5 degrees, then the difference between this assumption and the actual contact locations results in a stiffness error

$$\mathbf{E} = \begin{bmatrix} 1.000 & 0 & 0 & 0 \\ 0 & 1.000 & 0 & 0 \\ 0.131 & -0.006 & 1.000 & 0 \\ 0 & 0.044 & -0.044 & 0.996 \end{bmatrix}.$$

Since our manipulator mechanism precludes the rotation of the finger tips as they manipulate the object, (see section 4.1 below) the top two rows of $\mathbf{E}$ are unchanged from the identity matrix. Therefore, the stiffness terms generating $f_x$ and $f_y$ in the actual stiffness matrix are the same as the desired values. On the other hand, the rotational stiffness and grasp force values are altered by off-diagonal coupling terms. This means that translational displacement of the object will cause the controller to generate a torque on the object and change the grasp force, even if $\mathbf{K}_{obj}$ is diagonal. This coupling is a result of inaccurately modeling the transmission of forces from the finger tips to the object due to errors in determining the contact location. In particular, since the actual grasp force is directed between the contact locations, incorrect contact location information will result in forces that couple into $\tau$. If the finger tips of this manipulator rotated during manipulation, as with many designs, then non-zero terms would also appear in the upper half of the $\mathbf{E}$ matrix, coupling translational forces.

### 3.3 Error sources and tactile sensing

As indicated above, tactile sensing can limit kinematic errors in stiffness control in two ways. The first is by eliminating uncertainty in initial object orientation. By detecting the contact location on the finger tips as the object is grasped, the object orientation can be determined. In some cases it may be possible to infer the global object shape and orientation without an a priori model, by using tactile sensing to find the local curvature of the object and then extrapolating the overall object shape [Fearing 1990a]. However, in many tasks which require object stiffness control, some knowledge of the object will be available: we need to know something about the grasped object in order to know what to do with it. This is particularly true for tasks that involve tool use or parts mating, where stiffness control is most useful. In the experimental peg insertion task presented below, the controller implicitly assumes that the object is parallel-sided, and so for the cylindrical finger tips, the sensed contact locations provide the object orientation information.

The second way that tactile sensing can limit kinematic errors in stiffness control is by tracking changes in the location of the contacts between the finger tips and the grasped object. Tactile sensing is not the only means of tracking these changes; if a mathematical model of the finger tip and the object is available, finger joint angle measurements can be used to infer the object location [Montana 1986]. This approach is reasonable for simple objects, but determining a mathematical model of an irregular object may pose computational challenges. Another requirement which limits the application

of Montana's approach is that the object surfaces must be smooth and differentiable. In addition, these model-based schemes require initial values for the contact locations and cannot detect object slips during manipulation.

Maekawa et al. [1995] introduced a scheme that eliminates the need for a mathematical model of the object by using tactile sensor-based contact localization by integrating the sensed displacements of contact location. The advantage of this approach is that it is straightforward to manipulate around sharp corners, and a mathematical model of the object is not required. Once again, however, some model of object shape must be available for many dexterous tasks.

## 4. Experimental hardware

To demonstrate the benefits of tactile sensing for stiffness control, we implemented a stiffness controller on a planar robot hand with tactile array sensors on the finger tips, and executed a peg insertion task.

### 4.1 Planar hand and task apparatus

The two-fingered planar robot hand is shown in Figure 3. Each finger has two degrees of freedom, and the workspace is roughly circular, 10 cm in diameter and oriented in the vertical plane. The manipulator uses brushless DC motors in a parallel link, direct drive configuration to eliminate backlash and reduce friction. One unique feature of this manipulator is that the parallel linkages maintain constant finger tip orientation. Further details of the manipulator design can be found in [Howe 1992].

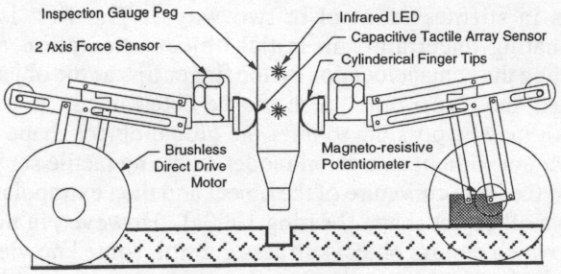


Figure 3. Two-fingered planar hand. The peg position and orientation is measured by tracking LEDs embedded in the peg with an optical position sensing device.

To capture the key aspects of a range of contact tasks where stiffness control is most useful, we selected a close-tolerance peg insertion task. The peg is a precision gauge pin, 12.70 mm in diameter, and the slot is constructed from machinist's parallels with a clearance less than 0.01 mm. The peg is mounted in a 2 cm wide handle with flat parallel sides. To permit independent measurement of the peg position and orientation, an optical tracker monitored the locations of two LEDs mounted in the peg handle.

### 4.2 Tactile array sensor

Tactile array sensors typically consist of a regular pattern of sensing elements to measure the distribution of pressure across the finger tip. The experiments reported here use capacitive tactile array sensors, based on an earlier design by Fearing [1990b]. These sensors consist of an 8x8 array of elements at 2 mm spacing in each direction, providing 64 force sensitive elements. The sensor is composed of two crossed layers of copper strips separated by thin strips of silicone rubber. The sensor forms a thin, compliant layer which can be easily attached to a variety of finger tip shapes and sizes. For these experiments, the 0.6 mm thick sensor is wrapped around a semi-cylindrical finger tip 25.4 mm in diameter, and covered with a 2.4 mm thick coating of silicone rubber; a photograph of the sensor is shown in Figure 4. Custom electronics scan the array to measure the capacitance at each element. The entire array is sampled by computer at 25 Hz, and gain and offset correction is applied to the reading from each element.

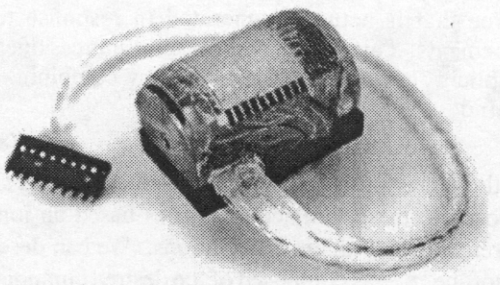

Figure 4. Capacitive tactile array sensor, 8 x 8 matrix at 2 mm spacing.

The tactile sensor signal can be processed to provide a great deal of information about the hand-object system. Among the parameters that can be extracted are contact location, object shape, and effective width of the pressure distribution. For the purposes of this experiment, we wish to extract the contact location for use by the controller. Many different algorithms can be used for this purpose; Son et al. [1995] compare three such schemes under real manipulation conditions. For this experiment, we have selected a thresholded centroid scheme. This algorithm only considers those elements which exceed a thresholded value. The benefits of this algorithm are that shear sensitivity is reduced, and the non-ideal pressure variations that occur during manipulation is smoothed.

## 5. Experimental results

### 5.1 Initial object orientation

The first experiment demonstrates the challenges in determining initial object orientation after grasping an object which is disturbed during the grasping process. The robot is commanded to grasp the peg, lift it, and rotate it in the vertical plane symmetric about the vertical axis. Because the peg is not placed exactly halfway between the fingers, one finger makes contact with the peg before the other. The base width of the pin is small compared with the height of the contact, so it can be tipped with less than 0.2 N of force.

The task is first performed without tactile sensing. Figure 5 shows the desired peg orientation, the controller's calculated peg orientation, and the actual peg orientation as measured by an optical tracker. The controller's peg orientation was calculated based on the assumptions that the object has flat parallel sides with a known object width, and that contact

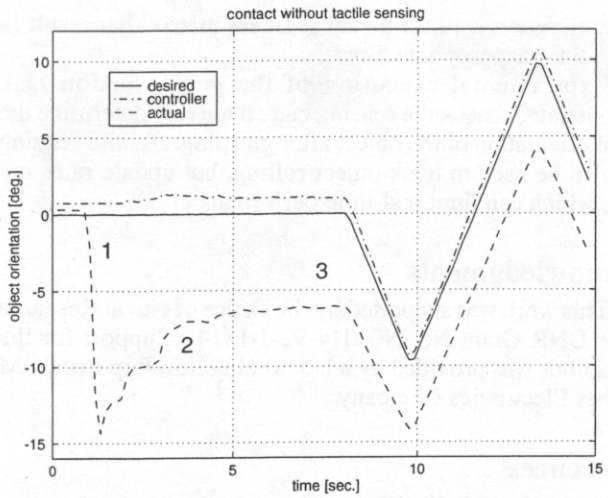


Figure 5. Peg orientation during grasp-lift-rotate task without tactile sensing. Events: (1) peg is tipped when one finger makes contact first; (2) actual and controller calculated peg orientation differ after lifting; (3) error persists due to lack of tactile sensing.

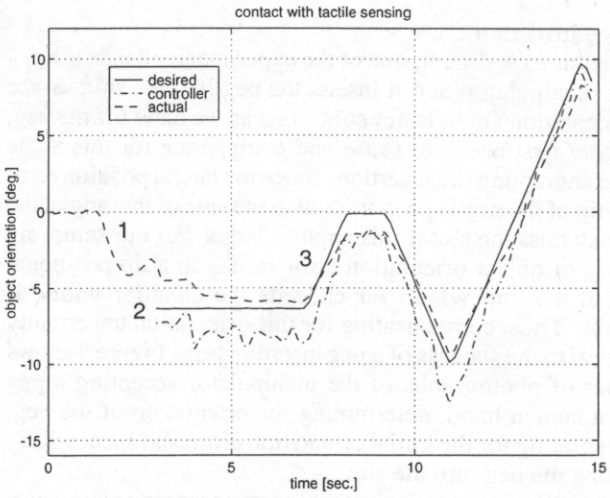


Figure 6. Peg orientation during grasp-lift-rotate task with tactile sensing. Events: (1,2) Peg is tipped again, but (3) tactile signals permit controller to roll the peg near the desired orientation.

occurs at $\phi = 0$. Although the finger tip force sensor is used to monitor contact forces in order to stop finger motion until the other finger makes contact, here the initial contact force is too low for the force sensor to work effectively, and the peg is tipped against the other finger, as indicated by event 1 in the figure.

The initial peg orientation of 14 degrees from vertical is reduced to about 6.5 degrees as the fingers close and the grasp force increases. This object orientation is stable after the grasp force enters the friction cones between the fingers and the object. The observed error is within the maximum orientation angle error of 10 degrees predicted by Figure 2. However, due to the absence of tactile feedback, the controller is unaware of this error, and it persists throughout the remainder of the task as the object is lifted and rotated. Increasing the controller gain does not reduce this kinematic error.

Figure 6 shows the same task, but here the orientation of the peg is determined from the tactile array sensor. Again, the peg is tipped before it is grasped, resulting in a significant deviation from the desired orientation. However, since the correct contact locations are determined through tactile sensing, the desired object orientation is maintained at the initial grasp orientation while the grasp force is increased. Through tactile sensing, the controller is able to compensate for this orientation error before the desired rotation trajectory is performed.

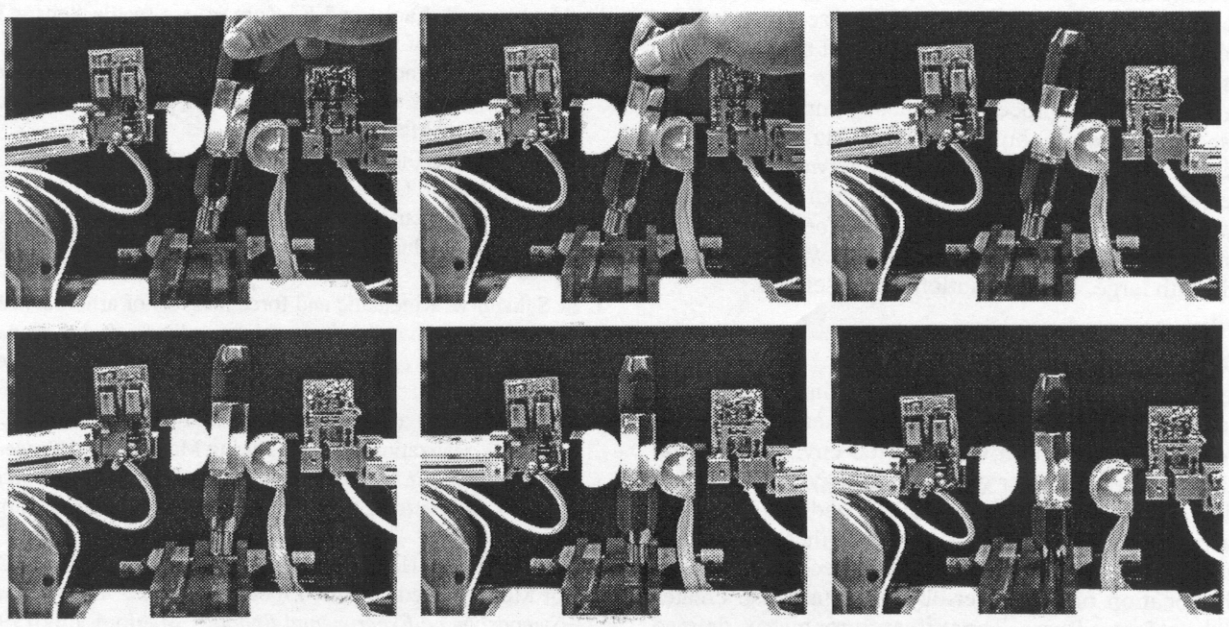

Figure 7. A sequence of photographs shows that a peg can be handed to the manipulator at an arbitrary angle, and the manipulator is able to sense the object orientation angle, compensate for it and perform the peg insertion task successfully.

### 5.2 Peg insertion

In this experiment, one of the experimenter hands the peg to the manipulator, and it inserts the peg into the slot. Since the orientation angle is not controlled as we hand off the peg, the robot first needs to sense and compensate for this angle before attempting the insertion. Since the lateral position error at the tip of the peg is proportional to the sine of this angle, the peg may miss the slot if this angle is large. For our setup, six degrees of object orientation error results in a tip positional error of 4.7 mm which far exceeds the chamfer width of 0.5 mm. Thus, compensating for this orientation uncertainty is critical to the success of a peg insertion task. Figure 7 shows a series of photographs of the manipulator accepting a peg from a human hand, determining the orientation of the peg, compensating for the initial orientation error, and successfully inserting the peg into the slot.

Due to limitations in the tactile array scanning electronics and the time required for sensor signal processing, the rate for determining the contact locations is currently limited to 25 Hz. This causes the contact location estimate to change in a discrete manner every 40 ms. Since the hand controller was running at a 500 Hz servo rate, the centroid signal was digitally filtered at 100 Hz using a one-pole low pass filter to smooth the discontinuities in the contact location signal and prevent abrupt transients in finger motion. When this contact centroid information was directly incorporated into the controller, the phase lag in the centroid information reduced the system bandwidth, so the stiffness gains could not be increased to the level possible without tactile feedback.

A second approach updates the tactile sensory information at 25 Hz, while using a small displacement model to interpolate between the sensed data points. This approach uses a tactile array sensor and a model of the object which does not require a priori knowledge of the object width which make it much more versatile than a model based scheme. The stiffness gain could be set higher than the previous filtered sensing method, but it did not approach that of the pure model based scheme.

It is possible to increase the array sensor sampling rate and decrease the signal processing time; an improved version of our sensor system should attain 200 Hz update rates. However, there is a fundamental tradeoff between increasing spatial resolution (i.e. number of array elements) and increasing update rates, which implies that techniques for incorporating slow sensory data into real-time controllers will be required for hands with large, high-resolution tactile sensors.

## 6. Conclusions

These results demonstrate that tactile information can improve the performance of object stiffness control for multifingered hands. In an unstructured environment, the orientation of an object after grasping can have considerable uncertainty. Under realistic manipulation conditions, analysis and experimental measurements show that these errors can pose significant limits to task execution. Imprecise information about the location of the finger-object contact also creates errors in the object stiffness. The stiffness error matrix, defined in equation (11) above, permits calculation of the effects of these grasp kinematic errors on object stiffness. This can result in coupling terms in the actual stiffness matrix that result in generating inappropriate forces.

Experimental execution of the peg insertion task demonstrated that tactile sensing can effectively determine the initial orientation of the object after grasping. Tactile sensing can also be used to track object rolling, but update rates are slow, which can limit real-time performance.

## Acknowledgments

This work was supported by the Office of Naval Research under ONR Grant No. N00014-92-J-1814. Support for the first author was provided by a Doctoral Fellowship from GM Hughes Electronics Company.

## References

A. D. Berger and P. K. Khosla. Using tactile data for real-time feedback. International Journal of Robotics Research, 10(2):88-102, April 1991.

N. Chen, H. Zhang, and R. Rink. Edge Tracking Using Tactile Servo. Proceedings of the 1995 IEEE/RSJ International Conference on Intelligent Robots and Systems, IROS '95. vol. 2, pages 84-89, Pittsburgh, PA, August 5-9, 1995.

M. R. Cutkosky and I. Kao. Computing and controlling compliance of a robotic hand. *IEEE Transactions on Robotics and Automation,* vol. 5, pages 151-165, April 1989.

R. S. Fearing. Tactile sensing for shape interpretation. In S. T. Venkataraman and T. Iberall, editors, *Dexterous Robot Hands.* Springer-Verlag, pages 209-238, 1990a.

R. S. Fearing. Tactile sensing mechanisms. *International Journal of Robotics Research,* 9(3):3–23, June 1990b.

R. Howe. A force reflecting teleoperated hand system for the study of tactile sensing in precision manipulation. *Proceedings of 1992 IEEE International Conference on Robotics and Automation,* pages 1321-1326, Nice, France, May 1992.

H. Maekawa, K. Tanie, and K. Komoriya. Tactile Sensor Based Manipulation of an Unknown Object by a Multifingered Hand with Rolling Contact. *Proceedings of the 1995 IEEE International Conference on Robotics and Automation,* pages 743-750, Nagoya, Aichi, Japan, May 21-27, 1995.

D. J. Montana. Tactile Sensing and the Kinematics of Contact. Ph.D. thesis, Harvard University. August 1986.

E. J. Nicolson. Tactile Sensing and Control of Planar Manipulator. Ph.D. thesis, University of California at Berkeley. November 1994.

J. K. Salisbury. Kinematic and force analysis of articulated hands. In M. T. Mason and J. K. Salisbury, editors, *Robot Hands and the Mechanics of Manipulation.* MIT Press, Cambridge, MA 1985.

J. S. Son, M. R. Cutkosky, and R. D. Howe. A Comparison of Contact Sensor Localization Abilities During Manipulation *Proceedings of the 1995 IEEE/RSJ International Conference on Intelligent Robots and Systems,* vol. 2 pages 96-103, Pittsburgh, August 5-9, 1995.

J. S. Son and R. D. Howe. Performance Limits and Stiffness Control of Multifingered Hands. *Proceedings of the 4th International Symposium on Experimental Robotics,* Stanford, July 1995.